

# Stochastic Noise Analysis of Neural Interface Front End

Amir Zjajo, Carlo Galuzzi, Rene van Leuken

Circuits and Systems Group  
Delft University of Technology  
Mekelweg 4, 2628 CD Delft, The Netherlands

**Abstract**— A time-domain methodology for noise analysis of neural interface front-end with arbitrary deterministic neuron model excitations is presented. Rather than estimating noise behavior by a population of realizations, the neural interface front-end is described as a set of stochastic differential equations and closure approximations are introduced to obtain the noise variances, covariances and cross-correlations between any electrical quantity and any stochastic source as a function of time. Statistical simulation shows that the proposed method offer an accurate and an efficient solution closely approximating those from a time-domain Monte Carlo analysis.

## I. INTRODUCTION

The recent trend in brain machine interfaces for neural electrophysiological recording [1] has largely been motivated by the growing interest in observing large scale neuronal activity. Quantifying noise in cellular dynamics and the physical electronic interface is one of the central challenges in the heterogeneous neural simulation and neural rehabilitation [2] including neural prosthetics and closed-loop stimulation strategies. Vast majority of the techniques proposed for noise analysis are frequency-domain techniques that are applicable to a particular circuit or a class of circuits. In time-domain, stochastic differential equations are proposed in [3] to obtain the time-varying covariance matrix of nonlinear circuits (e.g. oscillators in [4], PLLs in [5], discrete- and continuous-time circuits in [6]), and in [7], to obtain average and instantaneous power spectral density (PSD). In [6], a numerical methods for the efficient solution of stochastic differentials for noise analysis is proposed.

In this paper, we extend a time-domain, non-stationary stochastic noise analysis in [6] with a cyclo-stationary stochastic process to include the treatment of sampled data systems, and correspondingly, we derive the periodically time-varying spectral densities of such a process. In order to characterize the fundamental limits of the sensing process and post-processing interface circuit e.g. amplifier and A/D converter, we treat the neural cell noise fluctuations as homogeneous and inhomogeneous Markov chains and interface electronics noise as a non-stationary stochastic process. This approach provides key insight required to address signal-to-noise ratio (SNR), response time, and linearity of the physical electronic interface (i.e., saturation level).

## II. STOCHASTIC NOISE ANALYSIS

### A. Architectural Overview of an Integrated Neural Interface

The signal quality in neural interface front-end, beside the specifics of the electrode material and the electrode/tissue interface, is limited by the nature of the bio-potential signal and its biological background noise, dictating system resource constraints (power, size, bandwidth, and thermal dissipation i.e. to avoid tissue damage). The block diagram of a  $M$ -channel neural recording system architecture is illustrated in Figure 1. Due to the small amplitude of neural signals and the high impedance of the electrode tissue interface, amplification and low-pass filtering of the extracellular neural signals is performed before the signals can be digitized. An input-referred noise of an integrated front-end negative-feedback amplifier needs to be smaller than those of electrode and biological background noise. A successive approximation register (SAR)-based A/D converter digitizes the amplified neural signals with 10 bits of resolution. A low-power monolithic digital signal processing (DSP) unit provides additional filtering and executes a spike discrimination and sorting algorithms. The relevant information is then transmitted to an outside receiver through the transmitter or used for  $K$ -channel stimulation in a closed-loop framework.

### B. Noise Models

*Neural cell noise model:* In the Hodgkin and Huxley framework, a neural channel's configuration is determined by the states of its constituent subunits, where each subunit can be either in an open or closed state [8]. Adding a noise term  $\chi_x(V, t)$  ( $x=m, h$ , or  $n$ ) to the deterministic ordinary differential equation (ODE) of Hodgkin and Huxley is consistent with the behavior of the Markov process for channel gating [9]. Such process can be contracted to a Langevin description (via a Fokker-Planck equation) and expressed as delta-correlated noise processes  $\Gamma_{neuron}(t+\tau, t) = 1/\kappa[\alpha_x(1-x)+\beta_x x]\delta(\tau)$ , where  $\kappa$  is the total number of neural channels, and the transition rates  $\alpha_x(t)$  and  $\beta_x(t)$  are instantaneous functions of the membrane potential  $V(t)$ . Dirac's delta function  $\delta$  designates that the noise at different times is uncorrelated and the variables  $m$ ,  $h$ , and  $n$  represent the aggregated fraction of open subunits of different types, aggregated across the entire cell membrane.

---

This research was supported in part by the European Union and the Dutch government as part of the CATRENE program under Heterogeneous INCEPTION project.

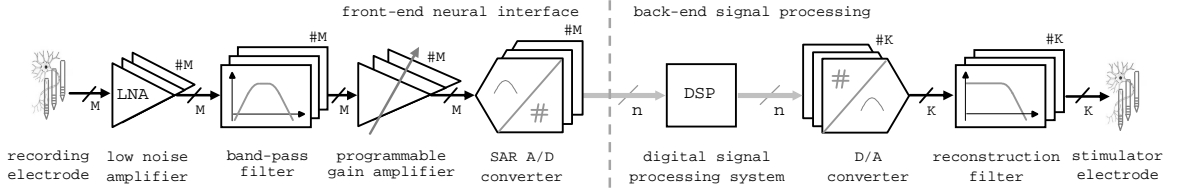


Figure 1: Block diagram of a brain machine interface with front-end neural interface and back-end signal processing of an integrated neural implant.

*Electrode-tissue interface noise model:* The overall noise of an electrode-tissue interface has contributions from the tissue/bulk thermal noise, the electrode-electrolyte interface noise, and the electronic noise. The most important types of electrical noise sources (thermal, shot, and flicker noise) in passive elements and integrated circuit devices have been investigated extensively, and appropriate models derived [10] as stationary and in [3] as nonstationary noise sources. We adapt model descriptions as defined in [3], where thermal and shot noise are expressed as  $\Gamma_{thermal}(t+\tau, t) = 2kTG(t)\delta(\tau)$  and  $\Gamma_{shot}(t+\tau, t) = qI_D(t)\delta(\tau)$ , respectively, where  $k$  is Boltzmann's constant,  $T$  is the absolute temperature,  $G$  is the conductance,  $q$  is the electron charge, and  $I_D$  is the current through the junction. These noise processes correspond to the current noise sources, which are included in the models of the integrated circuit devices. Tissue noise is modelled as the thermal noise generated by the solution/spreading or tissue/encapsulation resistance [11] and the electrode noise is the thermal noise generated by the charge transfer resistor [12]. The noise of the recording electronic circuits is mainly determined by the thermal and flicker noise generated by the input amplifier. Although the preamplifier can provide first-order low-pass filtering, dedicated low-pass filters are used to further minimize high-frequency noise. The cut-off frequency of low-pass filters is set to  $f_{Neuron} = 10$  kHz, where  $f_{Neuron}$  is the signal bandwidth of the action potential.

*A/D converter noise model:* Sampled data systems operate on the series of discrete-time samples taken at the end of the sampling period. Although the details of the processing during each period result in nonstationary noise voltages and currents, the same operation is performed each clock cycle, leading to the same signal statistics each clock cycle. Consequently, such stochastic process can be described as wide-sense cyclostationary. The special case of a white noise input source is of particular importance since the majority of the noise sources can be traced back to white noise generated in circuit components. For a white noise step input, the autocorrelation is a delta function, where  $S_{x_0}$  is the one-sided white noise power spectral density (PSD) of the underlying noise process. By using Parseval's theorem, the variance of the output as a function of the autocorrelation simplifies to  $\Gamma(t+\tau, t) = 1/2S_{x_0}(t)\delta(\tau)$  [13]. The one-sided noise PSD of the sampled output can then be found from the sum of the filtered and shifted two-sided input noise PSD  $S_x(f)$  [14]. Measurements of the output codes for a dc input signal to the A/D converter can be used to obtain an input-referred noise PSD estimate,

$S_{ADC}(f)$ . The noise of the input sampler and the converter quantization noise add to the input-referred noise PSD to give the total input noise PSD  $S_{total}(f) = S_{sample}(f) + S_{ADC}(f) + S_q(f)$ , where  $S_{sample}(f) = (kT/C_s)/(f_s/2)$  is the noise PSD from the input sampler over the Nyquist range ( $0 \leq f_{Neuron} \leq f_s/2$ ) and  $S_q(f) = (V_{LSB}^2/12)/(f_s/2)$  is the A/D converter quantization noise.

### C. Spectral Density and Time-Varying Variance

Consider description of the front-end neural interface with a system of stochastic differential equations

$$\mathbf{F}(\mathbf{r}, \mathbf{r}, t) + \mathbf{B}(\mathbf{r}, t) \cdot \boldsymbol{\chi} = 0 \quad (1)$$

where  $\mathbf{r}$  is the vector of stochastic processes that represents the state variables  $r(t)$  (e.g. node voltages), and  $\mathbf{B}(\mathbf{r}, t)$  is state and time dependent modulation for the vector of noise sources.  $\boldsymbol{\chi}$  is a vector of white Gaussian processes  $\chi(t)$  i.e. the derivative of the standard Wiener processes with the autocorrelation function given by  $\Gamma(t+\tau, t) = \mathbb{E}[\chi(t+\tau)\chi(t)]$ . Since noise is treated as a perturbation, a system of nonlinear stochastic differential equations in (1) is piecewise-linearized with  $\boldsymbol{\lambda} = [(\mathbf{r} - \mathbf{r}_0)^T, (\boldsymbol{\chi} - \chi_0)^T]^T$ ; the partial results are then combined to obtain the desired approximation. We will interpret (1) as an Itô system of stochastic differential equations. Such definition is consistent with the Markov process for neural channel gating with continuous sample rates. Using the multidimensional Itô formula, the variance matrix  $\mathbf{K}(t)$  of  $\boldsymbol{\lambda}(t)$  is expressed in differential Lyapunov matrix form as

$$d\mathbf{K}(t)/dt = \mathbf{E}(t)\mathbf{K}(t) + \mathbf{K}(t)\mathbf{E}(t)^T + \mathbf{B}(t)\mathbf{B}(t)^T \quad (2)$$

where  $\mathbf{E}(t) = \mathbf{F}'(\cdot)$  and  $K_{ij}(t) = \mathbb{E}[\lambda_i(t)\lambda_j(t)^T]$ , with the time-varying spectral, cross-spectral density matrix  $S_i(t, f) = \mathcal{F}\{K(t, \tau)\}$ . Correspondingly, the instantaneous periodically time-varying spectral densities  $S(f)$  of the cyclostationary stochastic process i.e. in A/D converters, can be expressed as the derivative with respect to time of the expected noise PSD

$$d\mathbf{K}'(t)/dt = \mathbf{E}(t)\mathbf{K}'(t) + \mathbf{K}(t)\exp(j\omega t) \quad (3)$$

where the elements of the vector  $K_i' = \mathbb{E}\{\lambda_i(t)R(t, \omega)^*\}$  [15], and  $R(t, \omega)$  is the Fourier transform of a  $t+\tau$ -segment of the noise waveform. To solve the system in (3), we need to calculate the time-varying transfer functions from the noise source  $\chi(t)$  to the components of  $r(t)$ , as defined in (2). To obtain a numerical solution, (2) has to be discretized in time using a suitable scheme, such as any linear multi-step method, or a Runge-Kutta method. If backward Euler is applied to (2), the differential Lyapunov matrix equation is written in a

special form referred to as the continuous-time algebraic Lyapunov matrix equation

$$\mathbf{E}_r \mathbf{K}(t_r) + \mathbf{K}(t_r) \mathbf{E}_r^T + \mathbf{B}_r \mathbf{B}_r^T = 0 \quad (4)$$

$\mathbf{K}(t)$  at time point  $t_r$  is calculated by solving the system in (4). In the circuit analysis, the matrix  $\mathbf{E}_r$  is, in general, not a full-rank matrix; it may have zero rows and columns, and, similarly, the node equation corresponding to this node will not contain any time-derivatives. Consequently, we rewrite (4) as a sparse linear matrix-vector system in standard form and solve it with adjusted alternating direction method

$$K_i = (\mathbf{E}_r^T - \gamma_i \mathbf{I}_n)(\mathbf{E}_r^T + \gamma_i \mathbf{I}_n)^{-1} K_{i-1} (\mathbf{E}_r - \gamma_i \mathbf{I}_n)(\mathbf{E}_r + \gamma_i \mathbf{I}_n)^{-1} - 2\gamma_i (\mathbf{E}_r^T + \gamma_i \mathbf{I}_n)^{-1} \mathbf{B}_r \mathbf{B}_r^T (\mathbf{E}_r + \gamma_i \mathbf{I}_n)^{-1} \quad (5)$$

for iterates  $i = 1, 2, \dots$ . This method generates a sequence of matrices  $\mathbf{K}_i$ , which converges fast towards the solution for sparse matrices with small bandwidth [16], provided that the iteration shift parameters  $\gamma_i$  are chosen (sub)optimally. Since iteration starts with  $\mathbf{K}_0 = 0$ ,  $\mathbf{K}_i$  will have rank at most  $i \times n$ , where  $n$  is the number of vectors in  $\mathbf{B}_r$ . As a result, a sequence of matrices  $\mathbf{K}_i$  needs only to be represented by less than  $i \times n$  vectors.

### III. EXPERIMENTAL RESULTS

The proposed method allows for any deterministic neuron model, whose neural conductance is described by a Markov process, to be converted into an equivalent stochastic version without involving any heuristics on the choice of the parameters for extra noise sources. The covariance matrix is periodic with the same period as either the input signal (e.g., translinear amplifier) or the clock (in sampled data systems). Moreover, with the proposed method, it is also possible to compute all the cross-correlations between any electrical quantity and any stochastic source. This makes it possible for the designer to determine the fundamental limit of the system's dynamic range, so that design efforts can be addressed to the most critical section of the circuit and avoid deteriorating power and chip area by overdesign. All the experimental results are carried out on a single processor Ubuntu Linux 9.10 system with Intel Core 2 Duo CPUs 2.66 GHz processor and 6 GB of memory. The proposed method and all sparse techniques have been performed in a numerical computing environment [17].

In time domain, a widespread approach for noise simulation is Monte Carlo (MC) analysis. However, accurately determining the noise requires a large number of simulations, so consequently, the Monte Carlo based methods become cpu-time consuming in complex, multichannel neural interface. The time series representation of a neuron signal at the preamplifier's input (Figure 2) are composed of a spike burst, plus additive Gaussian white noise (Figure 3, grey area with 1000 randomly selected neural channel compartments and black area with filtered out predicted bias from the estimated variance  $\sigma^2$ ). Difference in standard deviation of the proposed method vs. Monte Carlo analysis for 1000 iterations is within

5%; *cpu*-time is reduced from 2 hours to 46 sec for 25 ms of model time. Figure 4 illustrates the number of iteration steps. After low- and high-pass filtering and amplification, the noisy neural signal is sampled with SAR A/D converter. An example of the time-domain noise estimation and noise power spectral density at the output of the low-pass filter is illustrated in Figure 5 and Figure 6, respectively. For frequencies higher than  $\sim 10$  kHz, capacitances at the interface form the high-frequency pole and shape both the signal and the noise spectrum; the noise is low-pass filtered to the recording amplifier inputs. The interface's input equivalent noise voltage decreases as the gain across the amplifying stages increase (Figure 7), e.g. the ratio of the square of the signal power over its noise variance can be expressed as  $\text{SNR} = F_\Sigma^2 / (\sigma_{neural}^2 + \sigma_{electrode}^2 + \sum_i (\Pi_j G_j^{-1}) \sigma_{amp,i}^2)$ , where  $F_\Sigma$  is the total signal power,  $\sigma_{amp,i}^2$  represents the variance of the noise added by the  $i$ th amplification stage with gains  $G_j$ ,  $\sigma_{electrode}^2$  is the variance of the electrode and  $\sigma_{neural}^2$  is variance of the biological neural noise. The observed SNR of the system also increases as the system is isomorphically scaled up, which suggests a fundamental trade-off between SNR and speed of the system.

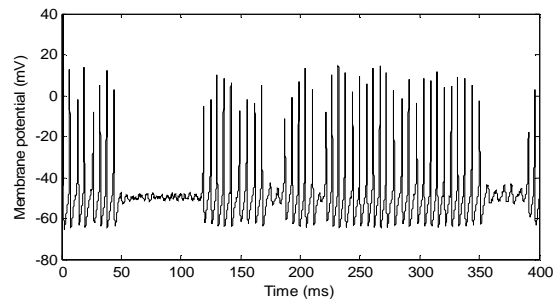


Figure 2: Nominal (without noise) voltage trace of neuron cell activity; the complex spike burst is followed by a pause in spike activity.

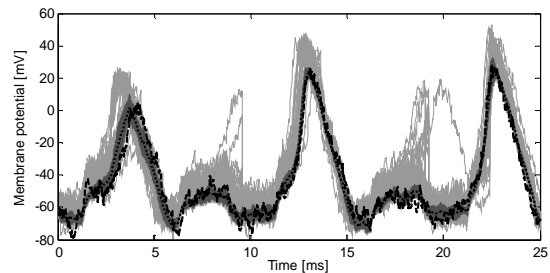


Figure 3: Statistical voltage trace of neuron cell activity; grey area - voltage traces from 1000 randomly selected neural channel compartments, black area - expected voltage trace.

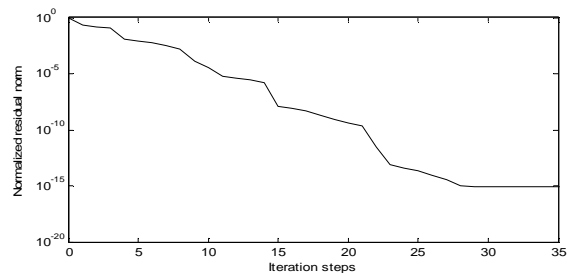


Figure 4: Stopping criterion: maximal number of iteration steps.

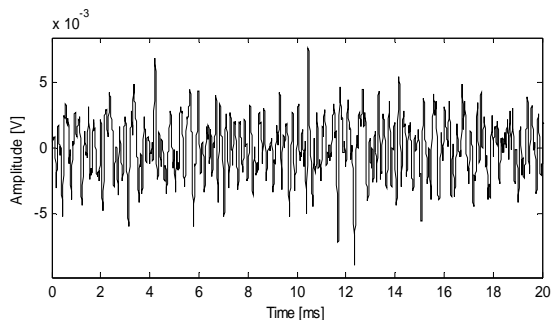


Figure 5: Noise amplitude in time-domain at the output of the low-pass filter; in comparison with 1000 Monte Carlo trials, the accuracy is within 3.2% with 21-fold *cpu*-time reduction.

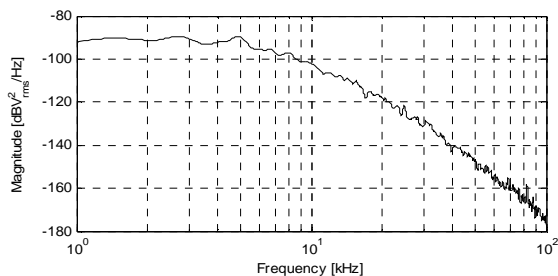


Figure 6: Noise PSD at the output of the low-pass filter.

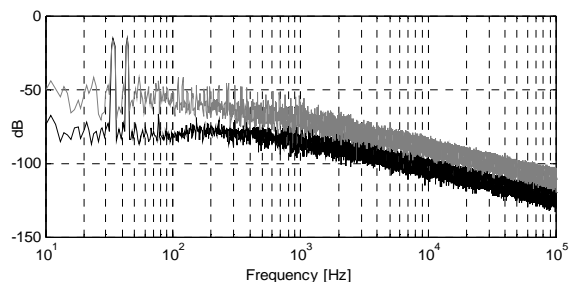


Figure 7: Spectral signature of SAR A/D converter-two tone test; black area – spectral content with nominal gain, grey area – spectra with 20% gain reduction, equivalent to 4 LSB loss in the dynamic range.

Design	Area [mm <sup>2</sup> ]	SNR (100Hz-10kHz) [dB]/channel				
		WCD slow, nom, fast [dB]	MC [dB]	SNA rel.	<i>t(cpu)</i> rel.	
LNA	0.096	58.5, 60.9, 62.5	58.9	4.3	35.4	
LPF	0.052	57.1, 58.9, 59.6	58.1	3.2	21.7	
HPF	0.066	56.3, 58.2, 59.7	56.9	4.1	23.4	
PGA	0.058	59.3, 60.7, 61.4	60.2	5.6	43.4	
SAR <sub>comp</sub>	0.036	56.7, 58.7, 59.4	57.4	2.9	17.2	
R <sub>DAC</sub>	0.074	57.9, 60.7, 61.6	59.3	6.2	24.6	
SAR <sub>logic</sub>	0.042	62.5, 64.6, 65.6	63.7	4.3	32.3	
Total	0.424	55.4, 57.3, 58.3	56.9	6.4	38.8	
Average				4.6	29.6	

TABLE I – SUMMARY OF THE ALGORITHM PERFORMANCE

In Table 1, SNR/channel estimated with worst-case analysis (WCD) and 1000 Monte Carlo (MC) iterations is compared across the neural interface circuits with the proposed stochastic noise analysis (SNA). Our approach allows large *cpu*-time reduction, ranging from 17-fold to 43-fold, with 29-fold on average. Difference in standard deviation of SNA vs. Monte Carlo analysis is less than 4.7% on average.

## IV. CONCLUSION

In this paper, we solve the set of linear time-varying equations, including the noise content description to find the steady state value of the time-varying variance matrix. The variance matrix is periodic with the same period as either the input signal (e.g., translinear amplifier) or the clock (in sampled data systems). Moreover, we compute all the cross-correlations between any electrical quantity and any stochastic source and compute noise spectral density. In a neural interfaces with large biological noise, this makes it conceivable to determine the limit of the system's dynamic range, and avoid deteriorating power and chip area by overdesign.

## REFERENCES

- [1] F. Chen, A.P. Chandrakasan, V.M. Stojanovic, "Design and analysis of a hardware-efficient compressed sensing architecture for data compression in wireless sensors," *IEEE Journal of Solid-State Circuits*, vol. 47, no. 3, pp. 744-756, 2012.
- [2] R. Harrison, "The design of integrated circuits to observe brain activity," *Proceedings of IEEE*, vol. 96, no. 7, pp. 1203-1216, 2008.
- [3] A. Demir, E. Liu, A. Sangiovanni-Vincentelli, "Time-domain non-Monte Carlo noise simulation for nonlinear dynamic circuits with arbitrary excitations," *Proceedings of IEEE International Conference on Computer Aided Design*, pp. 598-603, 1994.
- [4] A. Demir, A. Mehrotra, J. Roychowdhury, "Phase noise in oscillators: A unifying theory and numerical methods for characterization," *IEEE Transactions on Circuits and Systems-I*, vol. 47, no. 5, pp. 655-674, 2000.
- [5] A. Mehrotra, "Noise analysis of phase locked loops," *IEEE Transactions on Circuits and Systems-I*, vol. 49, no. 9, pp. 1309-1316, 2002.
- [6] A. Zjajo, *et al.*, "Stochastic analysis of deep-submicrometer CMOS process for reliable circuits designs," *IEEE Transactions on Circuits and Systems-I*, vol. 58, no. 1, pp. 164-175, 2011.
- [7] V. Vasudevan, "A time-domain technique for computation of noise-spectral density in linear and nonlinear time-varying circuits," *IEEE Transactions on Circuits and Systems-I*, vol. 51, no.2, pp. 422-433, 2004.
- [8] A. Hodgkin, A. Huxley, "A quantitative description of membrane current and its application to conduction and excitation in nerve," *Journal of Physiology*, vol. 117, pp. 500-544, 1952.
- [9] R.F. Fox, Y.-N. Lu, "Emergent collective behavior in large numbers of globally coupled independently stochastic ion channels," *Physics Review E*, vol. 49, pp. 3421-3431, 1994.
- [10] P.R. Gray, R.G. Meyer, *Analysis and Design of Analog Integrated Circuits*, New York: Wiley, 1984.
- [11] A.C. West, J. Newman, "Current distributions on recessed electrodes", *Journal of the Electrochemical Society*, vol. 138, no. 6, pp. 1620-1625, 1991.
- [12] Z. Yang, Q. Zhao, E. Keefer, W. Liu, "Noise characterization, modeling, and reduction for in vivo neural recording," *Advances in Neural Information Processing Systems*, pp 2160-2168, 2010.
- [13] J.H. Fischer, "Noise sources and calculation techniques for switched capacitor filters," *IEEE Journal of Solid-State Circuits*, vol. 17, no. 4, pp. 742-752, 1982.
- [14] T. Sepke, P. Holloway, C.G. Sodini, H.-S. Lee, "Noise analysis for comparator-based circuits," *IEEE Transactions on Circuits and Systems-I*, vol. 56, no. 3, pp. 541-553, 2009.
- [15] L. Arnold, *Stochastic Differential Equations: Theory and Application*, New York: Wiley, 1974.
- [16] E. Wachspress, "The ADI minimax problem for complex spectra", *Applied Mathematical Letters*, vol. 1, pp. 311-314, 1988.
- [17] MatLab, <http://www.mathworks.com/>.